

# Annealing time effects on the surface morphology of C–Pd films prepared on silicon covered with SiO<sub>2</sub>

MIROSŁAW KOZŁOWSKI<sup>1\*</sup>, JOANNA RADOMSKA<sup>1</sup>, HALINA WRONKA<sup>1</sup>, ELŻBIETA CZERWOSZ<sup>1</sup>,  
PIOTR FIREK<sup>2</sup>, KAMIL SOBCZAK<sup>3</sup>, PIOTR DŁUŻEWSKI<sup>3</sup>

<sup>1</sup>Tele and Radio Research Institute, Ratuszowa 11, 03-450 Warszawa, Poland

<sup>2</sup>Warsaw University of Technology, Institute of Microelectronics and Optoelectronics,  
Koszykowa 75, 00-662 Warszawa, Poland

<sup>3</sup>Institute of Physics PAS, al. Lotników 32/46, 02-668 Warszawa, Poland

\*Corresponding author: miroslaw.kozlowski@itr.org.pl

Morphology changes of C–Pd films prepared in physical vapor deposition (PVD) process and next annealed in a temperature of 650 °C during different time were studied. These studies were performed with electron microscopy methods (scanning SEM and transmission TEM). It was found that not annealed films are flat and they are composed of grains with composite character and size of 100–200 nm. Pd nanocrystallite of a diameter of a few nanometers in some carbon matrix was placed in these grains. For annealed films, a formation of palladium nanograins with different sizes and shapes as well as a porous carbon matrix were observed. High resolution TEM investigation was used to determine a structure of all these grains. An increase in duration time of annealing process led to diminishing of the porosity of carbon matrix and a number of Pd grains situated on the film surface. It was also stated that covering of Si with SiO<sub>2</sub> layer prevents formation of palladium silicide.

Keywords: Pd, carbon, film, SEM, TEM.

## 1. Introduction

The surface morphology of the sensing layers closely influences the sensitivity of a gas sensor. Various groups have attempted to expand the surface area of the gas sensing layer using various photolithographic techniques and advanced materials such as carbon nanotubes or nanostructural films. Although these reports gathered considerable interest because of the faster response times of the resulting gas sensors, these materials present poor recovery periods at room temperature while sensing toluene, CO, CO<sub>2</sub>, NO<sub>x</sub>, hydrogen and other gases. Especially palladium is widely used as a sensing material because of its great affinity towards hydrogen [1–3] and other gases and compounds (e.g., as Pd nanoparticles incorporated into a polymer or

into carbon [4, 5]). For example, palladium nanoparticles attached to carbonaceous nanostructure (nanotubes, nanodiamond, graphene, *etc.*) could modify the surface and next they can cause a change of material sensing properties. This nanocomposite material (*i.e.*, carbon–Pd nanoparticles) for sensing purposes is often deposited on silicon. On the other hand, it is known that palladium and silicon form Pd–Si alloys. Such Pd–Si alloys have been widely investigated by various techniques, and several stoichiometric structures have been found in the alloys, such as PdSi, Pd<sub>2</sub>Si, Pd<sub>3</sub>Si, Pd<sub>4</sub>Si, Pd<sub>5</sub>Si, and Pd<sub>9</sub>Si<sub>2</sub> [6–8]. Additionally, some efforts have been made for the synthesis of Pd–C compound. Some authors reported that carbon atoms incorporated into Pd lattice form Pd–C solid solution [9] or metastable phase of palladium carbide with carbon atoms on interstitial sites of metallic lattice [10]. This metastable phase decomposes at 870 K in an inert atmosphere, at 420 K in H<sub>2</sub> and O<sub>2</sub> [11], at 610 K in an argon atmosphere or under vacuum and at 460 K in H<sub>2</sub> [12]. It was reported that at higher temperatures (1150 K) palladium is able to catalyze the graphitization of amorphous carbon [13]. In all these cases, it is proposed that carbon is located in the octahedral hole of *fcc* Pd lattice [10, 14]. Though there are many similar chemical and physical properties for carbon and silicon, no observation of a Pd–Si structure-like phase has been reported in the Pd–C system.

In this paper we report studies of the topography and morphology of carbonaceous–palladium films (C–Pd film) obtained by physical vapor deposition (PVD) method on silicon covered with SiO<sub>2</sub> layer and annealed at 923 K in Ar atmosphere with different duration time of heat treatment. This layer's role is to prevent formation of Pd–Si alloy. SEM studies showed that SiO<sub>2</sub> layer is thick enough to fulfill this role.

## 2. Experiment

C–Pd films were deposited on silicon substrate covered earlier with SiO<sub>2</sub> sub-layer. The physical vapor deposition (PVD) method was applied to obtain the film on silicon covered with SiO<sub>2</sub> layer with thickness of 380 nm. This covering substrate layer was obtained by “wet chemical oxidation” process. SiO<sub>2</sub> layer was formed in the reaction of O<sub>2</sub> + H<sub>2</sub>O mixture at a temperature of 1373 K going on for 50 minutes.

To obtain C–Pd film, the fullerene (99.95%) and palladium acetate were evaporated from two separated sources under a dynamic vacuum of 10<sup>-5</sup> mbar. Prepared PVD films were annealed in argon gas as neutral atmosphere (with flow rate 40 l/min). The oven

T a b l e 1. Annealing processes parameters (*T* – temperature of annealing, *t* – process duration time, *F<sub>Ar</sub>* – argon flow rate).

Sample number	<i>T</i> [K]	<i>t</i> [min]	<i>F<sub>Ar</sub></i> [l/h]
F0	–	–	–
F5	923	5	40
F15	923	15	40
F30	923	30	40

with 3 cm in diameter quartz tube was used. These films were annealed in a temperature of 923 K for 5, 15 and 30 min. Parameters of annealing process are gathered in Tab. 1. Sample described as F0 is C-Pd film prepared by PVD method. Samples described as F5, F15 and F30 are C-Pd films annealed for 5, 15 and 30 min, respectively.

SEM investigation was performed with the JEOL JSM-7600F field emission scanning electron microscope operating at 2 keV and 5 keV incident energy. Both secondary (SE) and low angle backscattered (LABE) electrons detection were applied for imaging the film. In all cases, cross-sectional studies were performed on fractures of samples. Transmission electron microscopy (TEM) investigations were carried out with the Titan 80-300 Cubed high resolution transmission electron microscope operating at 300 keV incident electron beam energy. The specimens for TEM studies were prepared by transferring the film from the substrate to a special 3 mm diameter microscope mesh.

### 3. Results and discussion

The surface of F0 film and its cross-section shows Fig. 1. Surface of C-Pd film is very smooth and only faint outlines of carbon grains with a diameter of about 100 nm are visible (Fig. 1a). Cross-section through the C-Pd film and substrate with a SiO<sub>2</sub> layer is shown in Fig. 1b. Thickness of C-Pd film is about 450 nm and SiO<sub>2</sub> layer is about 380 nm. Details of structure of each layer on SEM figures are not visible.

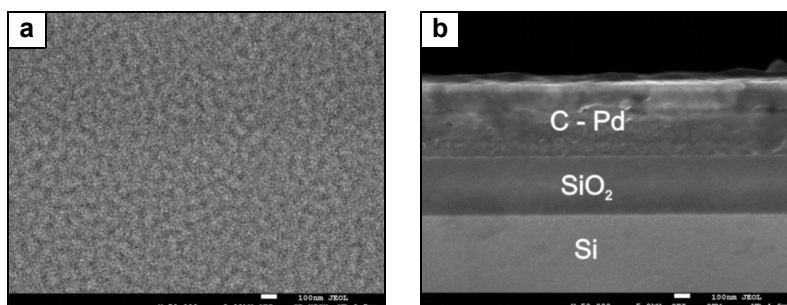


Fig. 1. Secondary electron images (SEI) of the surface of F0 film (a) and its cross-section (b).

Details of F0 film structure were revealed during high resolution transmission electron microscopy (HRTEM) investigations. In the carbonaceous matrix, small Pd nanoparticles with a diameter of few nanometers are visible (Fig. 2a). Many of them have a polycrystalline structure (Fig. 2b). Figure 2c shows a single palladium nanoparticle with *fcc* structure type and the marked distance between the planes of {111} Pd is estimated as 0.22 nm. The detailed analysis of TEM image leads to the observation of different interplanar distances and some stack defects within a volume of nanocrystallite (in regions marked with white circles). Such effects could be connected with defects generated by the incorporation of carbon atoms into Pd nanocrystallite.

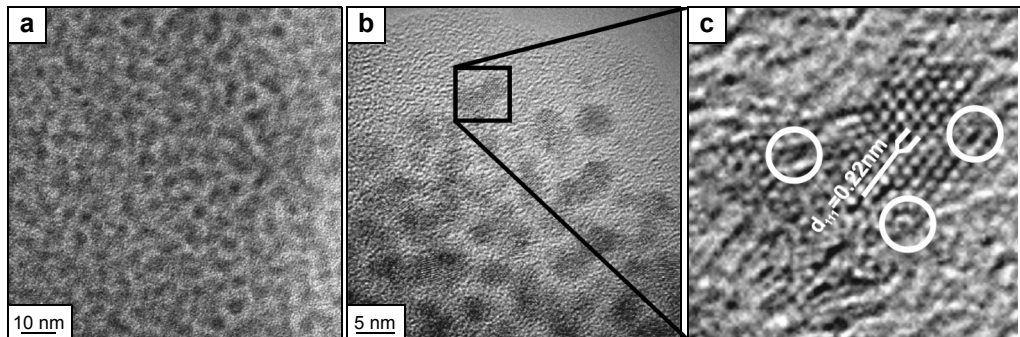


Fig. 2. TEM images of F0 composite film prepared in PVD process in different magnification (a, b), Pd nanoparticle with marked Pd {111} interplanar spacing (c).

Taking into account annealing temperature, such incorporation of carbon atoms into palladium lattice is possible, accordingly to the results of studies presented in [12, 13] of catalyzing by palladium of carbonaceous structure to amorphous carbon.

After annealing process, lasting 5 min, small palladium nanoparticles agglomerate into larger ones as well as these big nanograins form clusters of many grains with sizes up to few hundred nanometers. They are visible on the surface of the film (Figs. 3a and 3b) and on the cross-section of the film (Figs. 3c and 3d). The largest of them

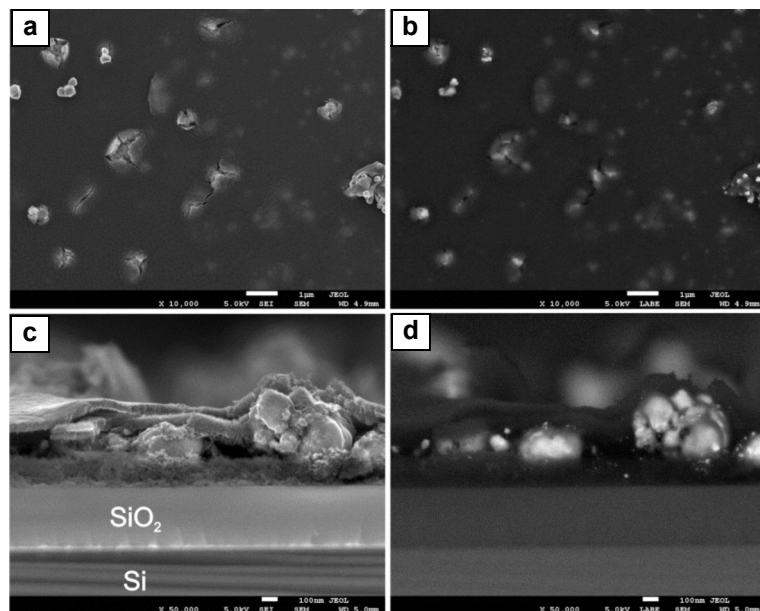


Fig. 3. SEM images of F5 film: SEI of surface (a), LABE image of surface (b), SEI of cross-section of film (c), LABE image of cross-section of film (d).

causes a local crack of carbonaceous matrix (Fig. 3a). A thin carbonaceous layer, which is visible on topmost of the film, has a thickness of about 45 nm (Fig. 3c). The analysis of SEM cross-sectional images made under LABE mode has shown that Pd nanoparticles agglomeration process in a short time of annealing (5 min) ran in the middle part of the film. In Figures 3b and 3d, Pd nanoparticles are visible as bright objects. In Fig. 3d, they are placed between two layers of dark carbonaceous matrix (above and below them). Pd grains with a few nanometers diameter are almost invisible in this dark carbonaceous matrix because of their too small diameter.

TEM investigations of F5 sample showed a large disparity in the size of palladium nanoparticles. The largest of them exceeded 200 nm (Fig. 4a), while the smallest had an initial diameter of a few nanometers (Fig. 4b). All nanoparticles of Pd are separated from each other. This indicates that 5 min annealing time was too short to allow for agglomeration of all Pd nanograins. Many of Pd nanoparticles are surrounded by graphite shells that are seen in Fig. 4c. The average thickness is about 10 nm, what means that Pd nanograins are surrounded by odd shells.

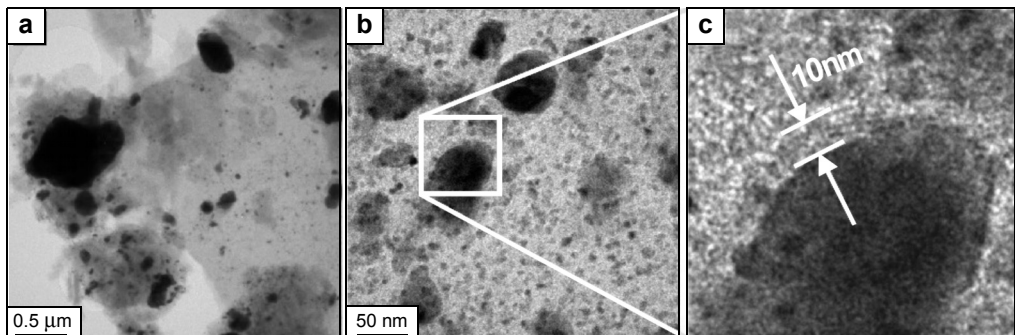


Fig. 4. TEM images of Pd nanoparticles with different diameter (a, b), graphite shells surrounding Pd nanoparticle (c).

In samples annealed for 15 min we found in SEM images Pd nanoparticles with different sizes. However, most of them are much smaller than in sample F5, although near the surface of the film some big grains with a length of more than 1  $\mu\text{m}$  are also seen (Fig. 5). Despite the longer time of annealing, a thin carbonaceous layer (with a thickness of about 45 nm) remains on the film surface, but its thickness is smaller than in the sample annealed for 5 min. SEM images of cross-section (Figs. 5c and 5d) of this sample show that the carbonaceous covering layer is free of Pd nanograins which are mainly placed at the bottom and in the internal part of the film.

TEM studies show that the agglomeration process has not been yet ended. These TEM images show big Pd nanoparticles with a diameter of tens of nanometers (Fig. 6a) and small with a diameter of several nanometers (Fig. 6b). In Figure 6a, some huge (with length of more than 1  $\mu\text{m}$ ) Pd grains are also observed. It seems that they agglomerate of smaller Pd nanoparticles what is shown in Figs. 6c and 6d. It should

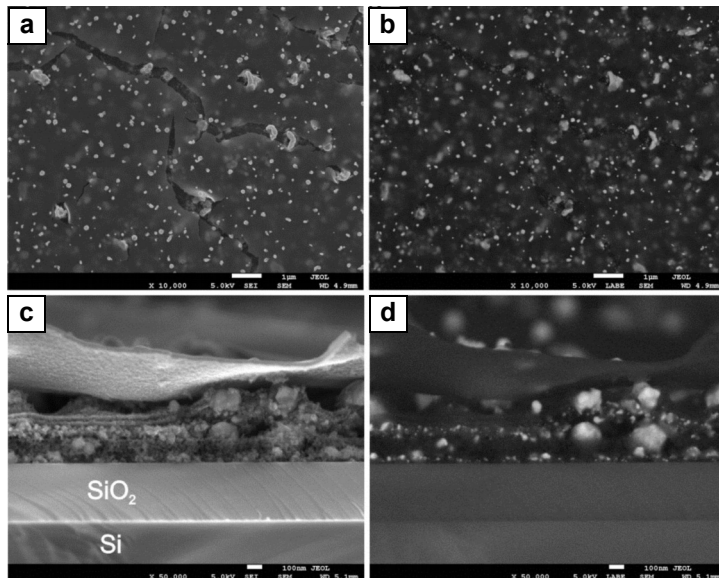


Fig. 5. SEM images of F15 film: SEI of surface (a), LABE image of surface (b), SEI of cross-section of film (c), LABE image of cross-section of film (d).

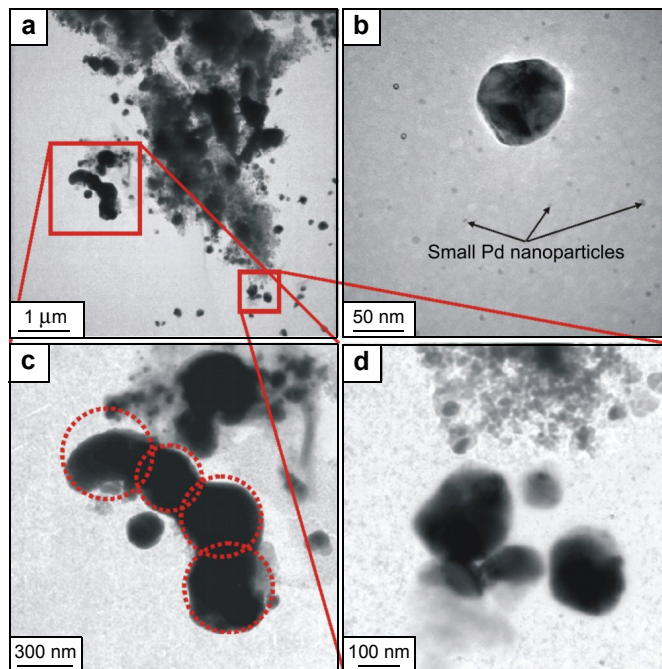


Fig. 6. TEM images for F15 sample (a), Pd nanoparticles with different diameter (b), Pd nanoparticles (circles indicated) forming huge Pd grains due to agglomeration process (c), Pd nanoparticles in earlier stage of agglomeration (d).

be also noticed that the situation registered in Fig. 6d could be an earlier stage of agglomeration, and this situation is illustrated in Fig. 6e. The observed nanograins are pure and no surrounding shells are seen.

Film annealed for 30 min still has a thin surface carbonaceous layer (Fig. 7a) which is much thinner than the one observed for sample F15 (less than 30 nm). It is almost invisible in the cross-section view (Fig. 7c). Pd nanoparticles are spread evenly over the entire thickness of the film (Figs. 7b and 7d). Circular cracks in this thin surface sub-layer are also found. From these cracks some longitudinal Pd grains are protruding (Figs. 7a and 7b). No small nanograins with few nanometers sizes Pd are anymore seen and carbonaceous matrix becomes more uniform and is not divided into sub-layers (Fig. 7d).

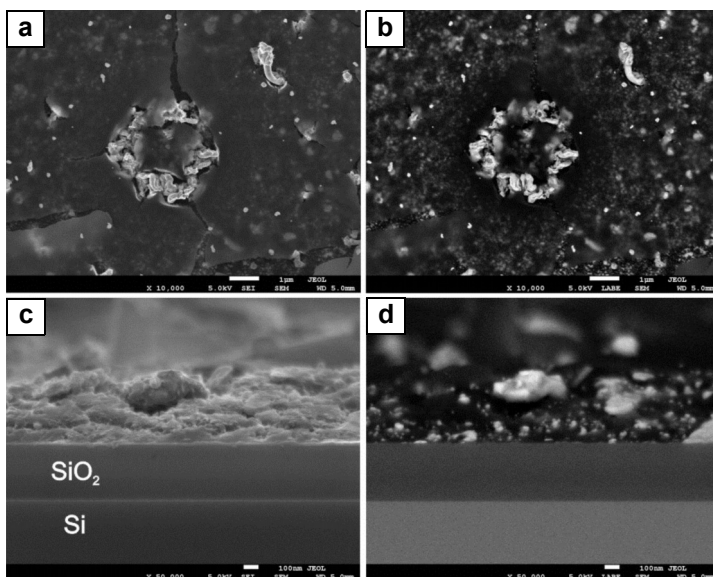


Fig. 7. SEM images of F30 film: SEI of surface (a), LABE image of surface (b), SEI of cross-section of film (c), LABE image of cross-section of film (d).

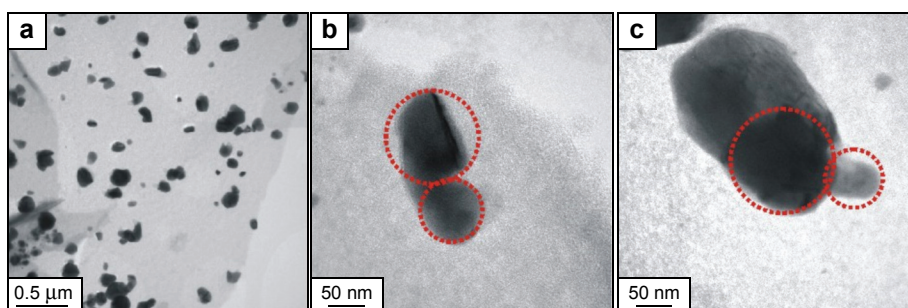


Fig. 8. TEM images of Pd nanoparticles with different diameter (a, b), formed agglomerates are presented (circles indicated) (b, c).

TEM observations of F30 samples show many Pd nanograins with a diameter from a few tens of nanometers up to a few hundred of nanometers, but none with a few nanometers in size (Fig. 8a). The final step in the agglomeration process of Pd nanoparticles was observed. The result of this process is shown in Fig. 8b and was marked by circles. No carbon shells were found for this sample.

## 4. Conclusions

Concluding, we can state that the film structure changes with annealing time, namely an increase in time causes a rise in a diameter of Pd nanograins, what could be connected with the agglomeration of Pd nanoparticles process. Due to the annealing process, the initially flat surface of the C–nPd film becomes rough and decorated with palladium nanoparticles or nanograins whose size increases with growing annealing time. Agglomeration and migration of Pd nanoparticles result in cracks and division of the film into sub-layers in which Pd nanograins with different sizes are situated.

It was also observed that carbon atoms could be incorporated into Pd lattice (especially on the edge of grains) forming a kind of C–Pd alloys.

*Acknowledgments* – The work was supported from European Regional Development Fund within the Innovative Economy Operational Programme 2007–2013 (project No. UDA-POIG.01.03.01-14-071/08-06).

## References

- [1] ARUNA I., MEHTA B.R., MALHOTRA L.K., *Faster H recovery in Pd nanoparticle layer based Gd switchable mirrors: Size-induced geometric and electronic effects*, Applied Physics Letters **87**(10), 2005, article 103101.
- [2] KUMAR P., MALHOTRA L.K., *Effect of current density on thermodynamic properties of nanocrystalline palladium capped samarium hydride thin film switchable mirrors*, Journal of Nanomaterials **2007**, 2007, article 52083.
- [3] LEWIS F.A., *The Palladium-Hydrogen System*, Academic Press, London, 2008, p. 1967.
- [4] SANTHOSH P., MANESH K.M., UTHAYAKUMAR S., KOMATHI S., GOPALAN A.I., LEE K.-P., *Fabrication of enzymatic glucose biosensor based on palladium nanoparticles dispersed onto poly(3,4-ethylene-dioxythiophene) nanofibers*, Bioelectrochemistry **75**(1), 2009, pp. 61–66.
- [5] ATTA N.F., EL-KADY M.F., GALAL A., *Palladium nanoclusters-coated polyfuran as a novel sensor for catecholamine neurotransmitters and paracetamol*, Sensors and Actuators B **141**(2), 2009, pp. 566–574.
- [6] NYLUND A., *Some Notes on the palladium-silicon system*, Acta Chemica Scandinavica **20**(9), 1966, pp. 2381–2386.
- [7] PFISTERER H., SCHUBERT K., *Neue Phasen Vom Mn<sub>p</sub>(B<sub>31</sub>)-Typ*, Zeitschrift für Metallkunde **41**, 1950, p. 358.
- [8] WYSOCKI J.A., DUWEZ P.E., *Equilibrium suicides of palladium*, Metallurgical and Materials Transactions A **12**(8), 1981, pp. 1455–1460.
- [9] MACIEJEWSKI M., BAIKER A., *Incorporation and reactivity of carbon in palladium*, Pure and Applied Chemistry **67**(11), 1995, pp. 1879–1884.

- [10] YAMAMOTO T., ADACHI M., KAWABATA K., KIMURA K., HAHN H.W., *Palladium carbide nanoparticles by gas flow reaction synthesis*, Applied Physics Letters **63**(22), 1993, pp. 3020–3022.
- [11] ZIEMECKI S.B., JONES G.A., SWARTZFAGER D.G., HARLOW R.L., FABER J., *Formation of interstitial palladium–carbon phase by interaction of ethylene, acetylene, and carbon monoxide with palladium*, Journal of the American Chemical Society **107**(15), 1985, pp. 4547–4548.
- [12] STACHURSKI J., FRACKIEWICZ A., *A new phase in the Pd–C system formed during the catalytic hydrogenation of acetylene*, Journal of the Less Common Metals **108**(2), 1985, pp. 249–256.
- [13] HOLSTEIN W.L., MOORHEAD R.D., POPPA H., BONDART M., [In] *Chemistry and Physics of Carbon*, Walker P.L. [Ed.], Vol. 18, Marcel Dekker, New York, 1982, p. 139.
- [14] KASZKUR Z., STACHURSKI J., PIELASZEK J., *X-ray diffraction study of the palladium–carbon system*, Journal of Physics and Chemistry of Solids **47**(8), 1986, pp. 795–798.

Received May 25, 2012